The Journal of Antibiotics (2018) 71:514–521
https://doi.org/10.1038/s41429-017-0016-9

JARA Japan Antibiotics Research Association
The Society for Actinomycetes Japan

ARTICLE

Time inside the mutant selection window as a predictor of staphylococcal resistance to linezolid

Kamilla N. Alieva[1] · Elena N. Strukova[1] · Maria V. Golikova[1] · Yury A. Portnoy[1] · Stephen H. Zinner[2] · Alexander A. Firsov[1]

Received: 9 August 2017 / Revised: 24 November 2017 / Accepted: 3 December 2017 / Published online: 18 January 2018

Abstract

To explore if the time inside the mutant selection window (T_{MSW}) is a reliable predictor of emergence of bacterial resistance to linezolid, mixed inocula of each of three methicillin-resistant *Staphylococcus aureus* strains (MIC of linezolid 2 μg ml^{-1}) and their previously selected resistant mutants (MIC 8 μg ml^{-1}) were exposed to linezolid pharmacokinetics using an in vitro dynamic model. In five-day treatments simulated over a wide range of the 24-h area under the concentration–time curve (AUC_{24}) to the MIC ratio, mutants resistant to 4 × MIC of antibiotic were enriched in a T_{MSW}-dependent manner. With each strain, T_{MSW} relationships with the area under the bacterial mutant concentration–time curve ($AUBC_M$) exhibited a hysteresis loop, with the upper portion corresponding to the time above the mutant prevention concentration (MPC; $T_{>MPC}$) of 0 and the lower portion—to the $T_{>MPC} > 0$. Using $AUBC_M$ related to the maximal value observed with a given strain (normalized $AUBC_M$) at $T_{>MPC} > 0$, a strain-independent sigmoid relationship was established between $AUBC_M$ and T_{MSW}, as well as $T_{>MPC}$ (r^2 0.99 for both). AUC_{24}/MIC and AUC_{24}/MPC relationships with normalized $AUBC_M$ for combined data on the three studied *S. aureus* strains were bell-shaped (r^2 0.85 and 0.80, respectively). These findings suggest that T_{MSW} at $T_{>MPC} > 0$, $T_{>MPC}$, AUC_{24}/MIC and AUC_{24}/MPC are useful bacterial strain-independent predictors of the emergence of staphylococcal resistance to linezolid.

Introduction

The emergence of bacterial resistance to antibiotics is the major contributor to their reduced efficacies [1]. Given a growing number of clinical reports on the isolation of resistant pathogens combined with a weak antibiotic pipeline [2], the development of new compounds is currently aimed at the suppression and/or restriction of resistance [3, 4]. Given that the enrichment of resistant mutants with concomitant loss in pathogen susceptibility should be concentration-dependent, concentration-resistance relationships are the methodological basis on which so-called "anti-mutant" antibiotic dosing regimens can be designed [5]. Such a relationship was first established in an in vitro study with fluoroquinolone-exposed *Staphylococcus aureus* using a dynamic model that simulates human antibiotic pharmacokinetics [6]. The loss in susceptibility of *S. aureus* occurred at intermediate but not at lower or higher antibiotic concentrations thereby exhibiting a bell-shaped relationship between bacterial resistance and the ratio of 24-h area under the concentration-time curve (AUC_{24}) to the MIC. This specific pattern of the AUC_{24}/MIC relationships with changing susceptibility of antibiotic-exposed *S. aureus* appeared to be consistent with the mutant selection window (MSW) hypothesis [7]. Since the MSW hypothesis predicts the enrichment of resistant mutants at antibiotic concentrations above the MIC, but below the mutant prevention concentration (MPC) the concentration-resistance relationship can be described by an extremum-containing function. This also has been confirmed in further in vitro studies with fluoroquinolones [6, 8–16], glycopeptides and lipopeptides [17], and oxazolidinones [18] that demonstrate bell-shaped relationships between the amplification of resistant mutants or loss in susceptibility of antibiotic-exposed bacteria and

Electronic supplementary material The online version of this article (https://doi.org/10.1038/s41429-017-0016-9) contains supplementary material, which is available to authorized users.

✉ Alexander A. Firsov
firsov@dol.ru

[1] Gause Institute of New Antibiotics, Moscow, Russian Federation

[2] Mount Auburn Hospital, Harvard Medical School, Cambridge, MA, USA

AUC_{24} or AUC_{24}/MIC. It was this ratio that allows prediction of strain-independent resistance thresholds, i.e., the "anti-mutant" AUC_{24}/MIC ratios, which were surprisingly less variable than the respective AUC_{24}/MPC ratios among fluoroquinolone-exposed Gram-negative bacteria [12, 15, 16] but not such exposed Gram-positive bacteria [19].

While AUC_{24}/MIC is commonly used to predict the emergence of bacterial resistance, the predictive potential of another parameter more closely linked with the MSW hypothesis—the time during which antibiotic concentrations are inside the MSW (T_{MSW}) remained uncertain until recently. Some studies have reported sigmoid relationships between T_{MSW} and the MIC elevations [6, 17, 20] or the enrichment of resistant mutants [17, 21, 22], whereas other studies [23–28] have not reported links between T_{MSW} and the emergence of resistance. Given the pharmacokinetic profile-dependent T_{MSW}-resistance relationships [20], conclusions about the low predictive power of the T_{MSW} drawn in some of the latter studies could have resulted from unjustified pooling of data obtained with different modes of antibiotic administration [23, 24], different dosing frequencies [27], and different half-lives of the same antibiotic [25]. However, even in those cases where T_{MSW}-resistance relationships were established, mutant enrichment better correlates with AUC_{24}/MIC than the T_{MSW} [6, 13, 17, 29]. The explanation for this variability was found only recently in our in vitro study with ciprofloxacin-exposed *Escherichia coli* [13]. When simulating ciprofloxacin pharmacokinetics over a wide range of the AUC_{24}/MIC ratio, T_{MSW}-resistance curves split into two portions, one for antibiotic concentrations below the MPC ($T_{>MPC} = 0$) and another for concentrations consistently above the MPC ($T_{>MPC} > 0$), exhibiting a hysteresis loop. Based on the separate data sets, the enrichment of resistant *E. coli* correlates better with T_{MSW} than for the entire data set ignoring $T_{>MPC}$.

To verify the same approach as applied to linezolid that has not been studied in this aspect, three methicillin-resistant *S. aureus* strains with different MPC/MIC ratios were exposed to linezolid pharmacokinetics over a wide range of the AUC_{24}/MIC ratio in five-day treatments simulated in an in vitro dynamic model. To ensure the presence of resistant cells at the start of simulated treatments, a mixed inoculum of the parent *S. aureus* strains and their linezolid-resistant mutants was used as described elsewhere [18].

Materials and methods

Antimicrobial agent and bacterial strains

Linezolid powder was kindly provided by Pfizer Inc. Three methicillin-resistant *S. aureus* strains including clinical isolates 479 and 688 and a well-characterized strain Mu50 (ATCC 700699) [30] and their previously selected linezolid-resistant mutants [18] were used in the study. The MIC of linezolid was 2 μg ml^{-1} for all three parent strains and 8 μg ml^{-1} for the resistant mutants. The MPCs of linezolid against *S. aureus* 479, *S. aureus* 688, and *S. aureus* ATCC 700699 regardless of the presence or absence of resistant mutants (mutation frequency 10^{-8}) were 5, 6, and 10 μg ml^{-1}, respectively [18].

Simulated pharmacokinetics and in vitro dynamic model

A series of monoexponential profiles that mimic twice-daily dosing of linezolid with a half-life of 6 h, in accordance with values reported in humans [31], was simulated for five consecutive days. The profiles were designed to provide ratios of AUC_{24}/MIC from 7.5 to 240 h with a stepwise two-fold increase. With each *S. aureus* strain this range covers the clinically attainable AUC_{24}/MIC ratio of ca. 120 h ($AUC_{24} = 228$ mg h l^{-1} divided by MIC = 2 μg ml^{-1}) [32].

A previously described dynamic model was used in the study [33]. Briefly, the model consisted of two connected flasks: one containing fresh Mueller-Hinton broth (MHB) and the other with a magnetic stirrer, a central unit, with the same broth containing a bacterial culture plus antibiotic (killing/regrowth experiments). Peristaltic pumps circulated fresh nutrient medium to the flasks and from the central 110-ml unit (initial 100 ml volume corrected by including additional 10 ml volume of the sampling system tubes) at a flow rate of 12.7 ml h^{-1}. Antibiotic dosing and specimen sampling of the central unit of the dynamic model were processed automatically using computer-assisted systems that provided sampling of each specimen from a separate port. The concordance between measured and designed linezolid concentrations has been reported elsewhere [18, 34].

The system was filled with sterile MHB and placed in an incubator at 37 °C. The central unit was inoculated with an 18-h culture of *S. aureus*. After a short incubation, the resulting exponentially growing cultures of linezolid-susceptible cells reached ~10^8 cfu ml^{-1} (10^{10} cfus per a 100 ml central unit) and 1 ml of a bacterial suspension of 10^2 cfu of resistant mutants was added to the central unit resulting in mutant content of one cell per 10^8 cfu of susceptible cells in 1 ml MHB to achieve a mutation frequency of 10^{-8}. A mixed inoculum of the parental cells and the resistant mutants was then exposed to linezolid administered as a bolus. The duration of each experiment was 120 h.

Population analysis

To determine viable counts of linezolid-susceptible and linezolid-resistant *S. aureus*, the central unit of the model

was multiply sampled throughout the observation period (120 h), and the samples were plated on Mueller-Hinton agar (MHA) without antibiotic and with 4× MIC of linezolid. The inoculated plates were incubated for up to 72 h at 37 °C and screened visually for growth. To minimize antibiotic carryover, samples were serially ≥10-fold diluted as appropriate and 100 µl was plated evenly onto MHA plates, which were incubated at 37 °C for 24 h. The lower limit of accurate detection was 2×10^3 cfu ml^{-1} (equivalent to 20 colonies of linezolid-susceptible plus linezolid-resistant cells per plate) and 10^2 cfu ml^{-1} (equivalent to at least one colony of linezolid-resistant cells per plate).

Based on population analysis data, areas under the bacterial mutant concentration-time curves $AUBC_M$s [19] were determined from the beginning of treatment to 120 h and were corrected for the area under the lower limit of quantification over the same time interval.

Relationships between $AUBC_M$ and MIC-related and MPC-related pharmacokinetic variables

$AUBC_M$s determined with individual *S. aureus* strains in each simulated treatment were plotted against four MIC-related and MPC-related pharmacokinetic variables: T_{MSW}, $T_{>MPC}$, and AUC_{24}/MIC and AUC_{24}/MPC ratios.

To ensure bacterial strain-independent prediction of the $AUBC_M$, combined data on the three *S. aureus* strains *versus* AUC_{24}/MIC or AUC_{24}/MPC and T_{MSW} or $T_{>MPC}$ were fitted with a modified Gaussian function:

$$Y = Y_0 + a\exp[0.5(|x - x_0|/b)^c], \quad (1)$$

where Y is $AUBC_M$, x is log (AUC_{24}/MIC) or log (AUC_{24}/MPC), Y_0 is the minimal value of Y, x_0 is log (AUC_{24}/MIC) or (AUC_{24}/MPC) that corresponds to the maximal value of Y, and a, b and c are parameters, and a sigmoid function:

$$Y = Y_0 + a/\{1 + \exp[-(x - x_0)/b]\}, \quad (2)$$

where Y is $AUBC_M$, x is T_{MSW} or $T_{>MPC}$, Y_0 and a are the minimal and maximal values of the $AUBC_M$, respectively, x_0 is x corresponding to $a/2$, and b is a parameter reflecting sigmoidicity.

All calculations were performed using SigmaPlot 12 software.

Results

In most simulated treatments, bacterial regrowth followed the initial decrease in density of the total population of linezolid-susceptible and linezolid-resistant *S. aureus* grown on antibiotic-free plates. At the intermediate AUC_{24}/MIC ratios (30–60 h), when mutants resistant to 4 × MIC of linezolid were enriched most intensively, their post-treatment numbers approached the sum of linezolid-susceptible and linezolid-resistant staphylococci. Typical time courses of viable counts observed for example with linezolid-exposed *S. aureus* 688 at one of the simulated AUC_{24}/MIC ratios are shown in Fig. 1.

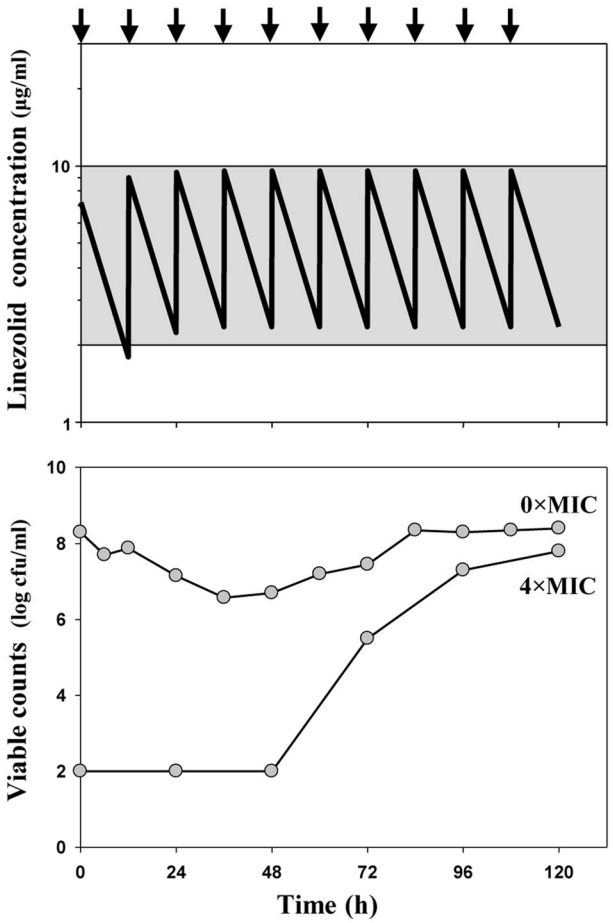

Fig. 1 Simulated pharmacokinetics of linezolid and time courses of surviving cells of *S. aureus* 688 grown on antibiotic-free plates (0 × MIC) and on plates containing 4 × MIC of linezolid. Simulated AUC_{24}/MIC ratio was 60 h. Antibiotic dosing is indicated by arrows. MSW is marked by the shaded area

A more detailed presentation of resistance data obtained with *S. aureus* 479, *S. aureus* 688, and *S. aureus* ATCC 700699 (Fig. 2) highlights T_{MSW}-dependent and AUC_{24}/MIC-dependent enrichment of linezolid-resistant mutants. At the smaller AUC_{24}/MIC ratios (7.5 and 15 h) when linezolid concentrations were below the MIC (T_{MSW} 0) or above the MIC for only 10% of the dosing interval, resistant mutants of *S. aureus* 479 and *S. aureus* ATCC 700699 were not enriched. With *S. aureus* 688 moderate mutant enrichment occurred only at the end of treatment. The most pronounced amplification of resistant staphylococci was observed at the AUC_{24}/MIC ratios of 30 (T_{MSW} 59% for all strains) and 60 h (T_{MSW} 52, 65, and 99% for *S. aureus* 479, *S. aureus* 688 and *S. aureus* ATCC 700699, respectively). At these AUC_{24}/MIC

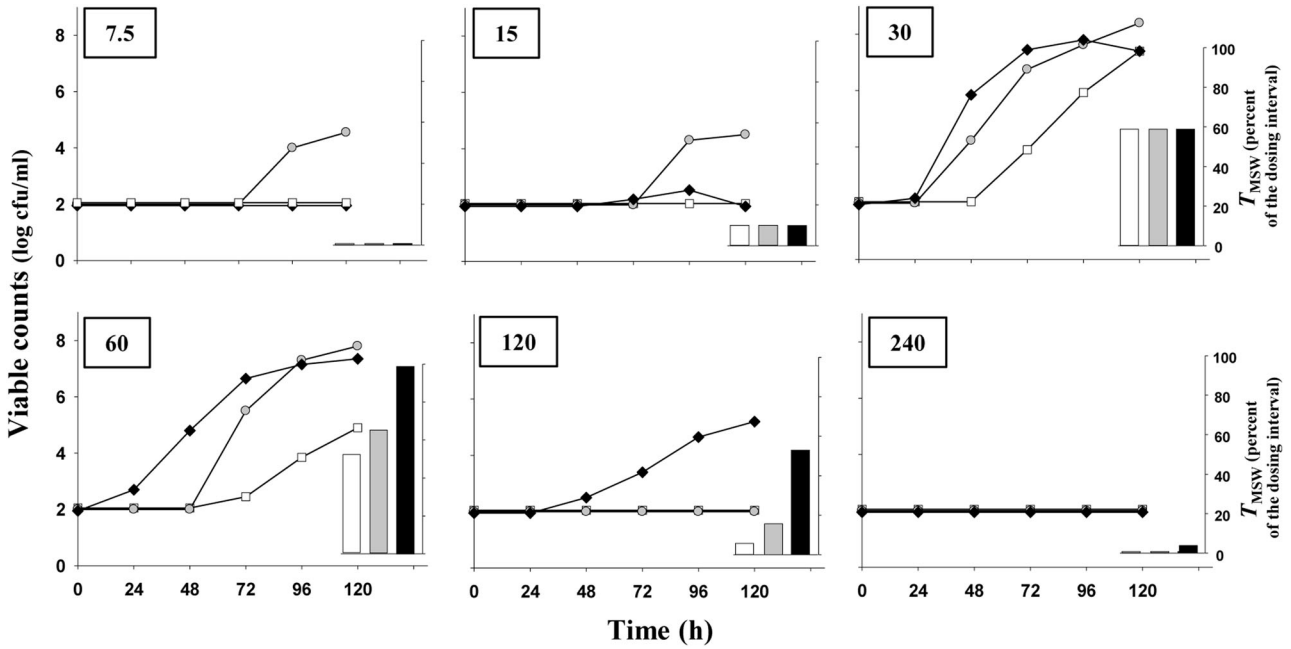

Fig. 2 Time courses of linezolid-resistant *S. aureus* subpopulations at different simulated AUC_{24}/MIC ratios (boxed numbers) and T_{MSW} values (bars). White squares and bars, *S. aureus* 479; gray circles and bars, *S. aureus* 688; black diamonds and bars, *S. aureus* ATCC 700699

ratios the number of resistant *S. aureus* ATCC 700699 mutants elevated significantly after 48 h from the start of the treatment and reached 8 log cfu ml^{-1} by 120 h. Substantial, but less than observed with *S. aureus* ATCC 700699 increase in the resistant *S. aureus* 688 cells was seen after 48 and 72 h at AUC_{24}/MIC ratios of 30 and 60 h, respectively, a day earlier than with *S. aureus* 479. Weaker and later growth was observed with *S. aureus* 479 resistant mutants. At the AUC_{24}/MIC ratio of 30 h their numbers were comparable to other strains only at the end of the observation period; at the AUC_{24}/MIC of 60 h maximal numbers with *S. aureus* 479 mutants were 1.5-fold lower than with *S. aureus* 688 and *S. aureus* ATCC 700699. There was no enrichment with resistant mutants at the highest simulated AUC_{24}/MIC ratio of 240 h (T_{MSW} 0% for *S. aureus* 479 and 688 or 4% for *S. aureus* ATCC 700699), while at the clinically achievable ratio of ca. 120 h moderate enrichment did occur with *S. aureus* ATCC 700699 (T_{MSW} 53%) but not *S. aureus* 479 and 688 (T_{MSW} 6 and 16%, respectively). Thus, the enrichment of resistant mutants of the studied *S. aureus* strains was AUC_{24}/MIC-dependent.

With each *S. aureus* strain, T_{MSW} plots of the $AUBC_M$ were qualitatively similar and they split into two parts (Fig. 3, left panel). The upper plots meet the condition of $T_{>MPC} = 0$, and the lower plots—$T_{>MPC} > 0$. This results in a hysteresis loop, more distinct with *S. aureus* 688 and, in particular, ATCC 700699 mutants than with *S. aureus* 479. Although $AUBC_M$ increased with an increase in T_{MSW} regardless of whether linezolid concentrations were above the MPC or not, the upper plots predict greater $AUBC_M$s than the lower plots at the same T_{MSW}. Using T_{MSW} of 50% of the dosing interval as a vertical intersecting line, the $AUBC_M$s for *S. aureus* 688, *S. aureus* 479 and *S. aureus* ATCC 700699 were respectively 1.6-fold, 1.9-fold, and 2.5-fold greater when linezolid concentrations did not reach the MPC ($T_{>MPC} = 0$) than at antibiotic concentrations which exceeded the MPC ($T_{>MPC} > 0$).

AUC_{24}/MIC relationships with $AUBC_M$ were bell-shaped with each *S. aureus* strain (Fig. 3, right panel). The $AUBC_M$ increased with an increase in the AUC_{24}/MIC, reaching a maximum, and then, at higher AUC_{24}/MICs, $AUBC_M$ decreased to zero. AUC_{24}/MPC relationships with $AUBC_M$ were similar. With each organism, the descending portion of the bell-shaped curve was associated with $T_{>MPC} > 0$. Like T_{MSW} plots, the patterns of the AUC_{24}/MIC-$AUBC_M$ curves were similar for all three *S. aureus* strains, but these curves were strain-specific in terms of the absolute $AUBC_M$ values: smaller with *S. aureus* 479, intermediate with *S. aureus* 688 and larger with ATCC 700699. For example, the respective maximal $AUBC_M$ values (205, 379, and 431 log cfu h ml^{-1}) observed at the same AUC_{24}/MIC ratio (30 h) varied in a more than two-fold range. For this reason, when combining data obtained with different *S. aureus* strains, the $AUBC_M$s were related to the maximal value observed with a given strain. As seen in Fig. 4a, b, Gaussian function (Eq. 1) fits the normalized $AUBC_M$-AUC_{24}/MIC, and $AUBC_M$-AUC_{24}/MPC data with high r^2s (0.85 and 0.80, respectively) that are higher than for the non-normalized data (0.36 and 0.65, respectively).

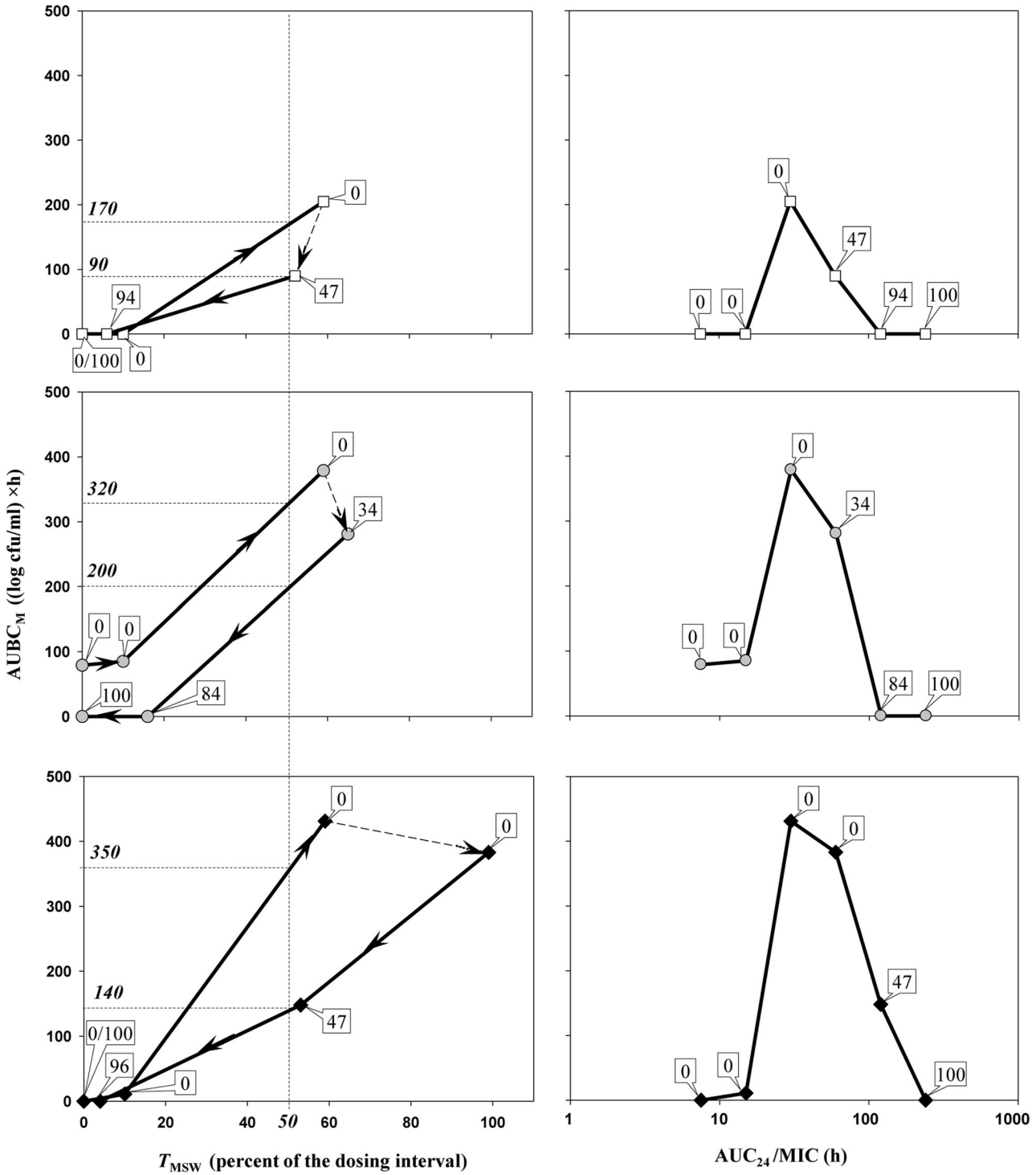

Fig. 3 T_{MSW} and AUC$_{24}$/MIC relationships with AUBC$_M$. $T_{>MPC}$ values are shown in callouts. White squares, *S. aureus* 479; gray circles, *S. aureus* 688; black diamonds, *S. aureus* ATCC 700699

Using normalized AUBC$_M$ belonging to the lower plots shown on the left panel of Fig. 3 ($T_{>MPC} > 0$), a strain-independent relationship between AUBC$_M$ and T_{MSW} was established (Fig. 4c). A sigmoid function (Eq. 2) fits combined data with the three *S. aureus* strains with high r^2 (0.99). For the points that meet the condition $T_{>MPC} > 0$ the sum of T_{MSW} and $T_{>MPC}$ equals 100% of the dosing interval, the $T_{>MPC}$ plot of the AUBC$_M$ (Fig. 4d) is a mirror image of the T_{MSW} plot with the same r^2. Thus, all four MIC-related and MPC-related pharmacokinetic variables are equally

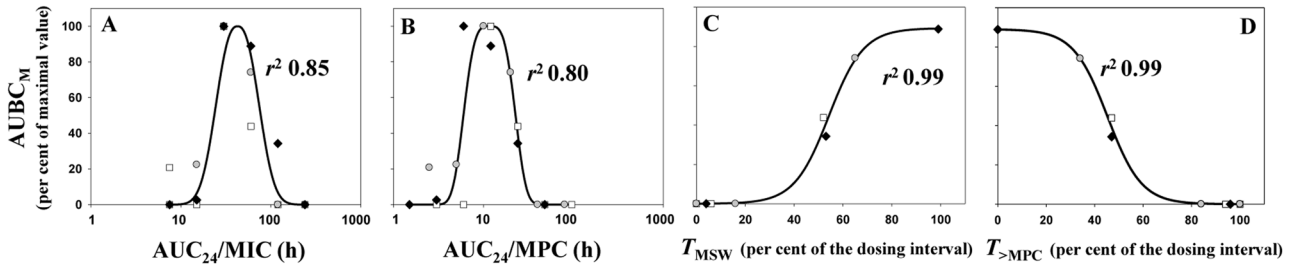

Fig. 4 AUC_{24}/MIC, AUC_{24}/MPC, T_{MSW}, and $T_{>MPC}$ relationships with $AUBC_M$ (combined data on three *S. aureus* strains) fitted by Eq. (1): **a** $Y_0 = 0$, $a = 100.0$, $b = 0.2389$, $c = 2.392$, $x_0 = 1.630$; **b** $Y_0 = 0$, $a = 100.0$, $b = 0.2643$, $c = 3.518$, $x_0 = 1.066$) and Eq. (2): **c** $Y_0 = 0$, $x_0 = 54.22$, $a = 89.35$, $b = 7.101$; **d** $Y_0 = 0$, $x_0 = 45.28$, $a = 89.02$, $b = -7.026$). White squares, *S. aureus* 479; gray circles, *S. aureus* 688; black diamonds, *S. aureus* ATCC 700699

predictive of the emergence of staphylococcal resistance to linezolid.

Discussion

Using in vitro simulations of five-day treatments of linezolid-susceptible *S. aureus* supplemented by resistant mutants, their enrichment was shown to correlate with MIC-related and/or MPC-related pharmacokinetic variables. With each of the three studied strains T_{MSW} relationships of the $AUBC_M$ had the form of hysteresis, with the upper portion of its loop corresponding to $T_{>MPC} = 0$, whereas the lower portion to $T_{>MPC} > 0$. Because the sigmoid rise in the $AUBC_M$ with an increase in T_{MSW} was steeper at $T_{>MPC} = 0$ than at $T_{>MPC} > 0$, greater $AUBC_M$s were observed at a given T_{MSW} when linezolid concentrations were below the MPC than above the MPC. Recently, similar patterns have been reported in our study with ciprofloxacin-exposed *E. coli* [13]. These findings suggest the previously hypothesized idea of heterogeneity of the MSW that was tested by simulations of ciprofloxacin concentrations oscillating closer either to the MPC ("upper case") or the MIC ("lower case") at the same T_{MSW} [35]. The $AUBC_M$ in the upper case was shown three times smaller than in the lower case for two strains of ciprofloxacin-exposed *S. aureus*.

A distinct $T_{>MPC}$-dependent splitting of the $AUBC_M$-T_{MSW} curves makes combining data obtained at $T_{>MPC} = 0$ and at $T_{>MPC} > 0$ incorrect. It is no coincidence that Eq. (2) described $AUBC_M$-T_{MSW} data at $T_{>MPC} > 0$ (Fig. 4c) much better than the combined data at $T_{>MPC} = 0$ and at $T_{>MPC} > 0$ (r^2 0.99 versus r^2 0.24). It is very likely that the incorrect combination of data obtained at $T_{>MPC} = 0$ and at $T_{>MPC} > 0$ might contribute to the underestimation of the true role of the T_{MSW} as a predictor of the emergence of bacterial resistance. Apparently, this occurred in a resistance study with meropenem-exposed *Acinetobacter baumannii*: [28] with each of the studied strains, the T_{MSW}s observed at the minimal antibiotic exposure met the condition $T_{>MPC} = 0$, whereas the T_{MSW}s at the maximal exposure met the condition $T_{>MPC} > 0$.

As established in the present study, T_{MSW} at $T_{>MPC} > 0$ and $T_{>MPC}$ are equally predictive of the enrichment of resistant *S. aureus*: the shorter the T_{MSW} or the longer the $T_{>MPC}$, the less mutants. Therefore, $T_{>MPC}$ plot of the $AUBC_M$ (Fig. 4d) was a mirror image of the T_{MSW} plot (Fig. 4c) with the same r^2 (0.99); for the points that meet the condition $T_{>MPC} > 0$ the sum of T_{MSW} and $T_{>MPC}$ equals 100% of the dosing interval. However, this is true for antibiotics with long half-lives but not for shorter half-life agents such as beta-lactams. For example, even at the relatively high AUC_{24}/MIC ratios that prevent the amplification of resistant *Pseudomonas aeruginosa*, doripenem trough concentrations were lower than the MIC [29], and the sum of T_{MSW} and $T_{>MPC}$ was <100% of the dosing interval. In this light, T_{MSW} and $T_{>MPC}$ are not interchangeable.

Along with T_{MSW} and $T_{>MPC}$, two other indices, AUC_{24}/MIC and AUC_{24}/MPC can be bacterial strain-independent predictors of the selection of linezolid-resistant *S. aureus*. Given the pronounced inter-strain variability in the maximal value of the $AUBC_M$ but not in the slopes of the ascending and descending portions of the AUC_{24}/MIC- or AUC_{24}/MPC-$AUBC_M$ curves (Fig. 3), to combine data obtained with individual *S. aureus* strains, the $AUBC_M$s normalized by their maximal values were plotted against AUC_{24}/MIC and AUC_{24}/MPC (Fig. 4a, b). Both AUC_{24}/MIC and AUC_{24}/MPC relationships with the normalized $AUBC_M$ appeared to be strain-independent (r^2 0.85 and 0.80, respectively), and in this sense they are equally predictive of resistant mutant enrichment. Because of the small variability in the MPC/MIC ratio for the studied strains from 2.5 (*S. aureus* 479), and 3 (*S. aureus* 688) to 5 (*S. aureus* ATCC 700699), AUC_{24}/MIC and AUC_{24}/MPC could not be discriminated by their predictive potentials.

Given the increasing prevalence of antibiotic resistant pathogens and the relative paucity of new antibiotics in development, optimal antibiotic therapy should consider the suppression of resistance [1]. In this light, searching for

quantitative relationships between the enrichment of resistant mutants and MIC-related and MPC-related pharmacokinetic variables may be a basis for the development of "anti-mutant" antibiotic dosing. The establishment of dosing regimens that prevent or restrict mutant enrichment is critical for new antibacterial agents as well as for currently existing antibiotics.

Overall, the findings obtained in the present study support the MSW hypothesis [7] as applied to linezolid-resistant *S. aureus*.

Compliance with ethical standards

Conflict of interest The authors declare that they have no conflict of interests.

References

1. Bush K, et al. Tackling antibiotic resistance. Nat Rev Microbiol. 2011;9:894–6.
2. Butler MS, Blaskovich MA, Cooper MA. Antibiotics in the clinical pipeline in 2013. J Antibiot. 2013;66:571–91.
3. Lister P. The role of pharmacodynamic research in the assessment and development of new antibacterial drugs. Biochem Pharmacol. 2006;71:1057–65.
4. Abdul-Aziz MH, Lipman J, Mouton JW, Hope WW, Roberts JA. Applying pharmacokinetic/pharmacodynamic principles in critically ill patients: optimizing efficacy and reducing resistance development. Semin Respir Crit Care Med. 2015;36:136–53.
5. Firsov, AA, Zinner, SH, Lubenko, IY. In vitro dynamic models as tools to predict antibiotic pharmacodynamics. In: Nightingale, CH, Ambrose, PG, Drusano, GL, Murakawa, T, editors. Antimicrobial pharmacodynamics in theory and clinical practice. New York, NY: Informa Healthcare USA, Inc., 2007. p. 45–78.
6. Firsov AA, et al. In vitro pharmacodynamic evaluation of the mutant selection window hypothesis using four fluoroquinolones against *Staphylococcus aureus*. Antimicrob Agents Chemother. 2003;47:1604–13.
7. Zhao X, Drlica K. Restricting the selection of antibiotic-resistant mutants: a general strategy derived from fluoroquinolone studies. Clin Infect Dis. 2001;33:147–56.
8. Zinner SH, et al. Emergence of resistant *Streptococcus pneumoniae* in an in vitro dynamic model that simulates moxifloxacin concentrations inside and outside the mutant selection window: related changes in susceptibility, resistance frequency and bacterial killing. J Antimicrob Chemother. 2003;52:616–22.
9. Firsov AA, et al. ABT492 and levofloxacin: comparison of their pharmacodynamics and their abilities to prevent the selection of resistant *Staphylococcus aureus* in an in vitro dynamic model. J Antimicrob Chemother. 2004;54:178–86.
10. Tam VH, Louie A, Deziel MR, Liu W, Drusano GL. The relationship between quinolone exposures and resistance amplification is characterized by an inverted U: a new paradigm for optimizing pharmacodynamics to counterselect resistance. Antimicrob Agents Chemother. 2007;51:744–7.
11. Gebru E, Choi M-J, Lee S-J, Damte D, Park SC. Mutant prevention concentration and mechanism of resistance in clinical isolates and enrofloxacin/marbofloxacin-selected mutants of *Escherichia coli* of canine origin. J Med Microbiol. 2011;60:1512–22.
12. Firsov AA, et al. Bacterial resistance studies using in vitro dynamic models: the predictive power of the mutant prevention and minimum inhibitory antibiotic concentrations. Antimicrob Agents Chemother. 2013;57:4956–62.
13. Firsov AA, Portnoy YA, Strukova EN, Shlykova DS, Zinner SH. Predicting bacterial resistance using the time inside the mutant selection window: possibilities and limitations. Int J Antimicrob Agents. 2014;44:301–5.
14. Firsov AA, Strukova EN, Portnoy YA, Shlykova DS, Zinner SH. Bacterial antibiotic resistance studies using *in vitro* dynamic models: population analysis vs. susceptibility testing as endpoints of mutant enrichment. Int J Antimicrob Agents. 2015;46:313–8.
15. Strukova EN, et al. Searching for the optimal predictor of ciprofloxacin resistance in *Klebsiella pneumoniae* by using in vitro dynamic models. Antimicrob Agents Chemother. 2015;60:1208–15.
16. Strukova EN, Portnoy YA, Zinner SH, Firsov AA. Predictors of bacterial resistance using in vitro dynamic models: area under the concentration-time curve related to either the minimum inhibitory or mutant prevention antibiotic concentration. J Antimicrob Chemother. 2016;71:678–84.
17. Firsov AA, et al. Testing the mutant selection window hypothesis with *Staphylococcus aureus* exposed to daptomycin and vancomycin in an in vitro dynamic model. J Antimicrob Chemother. 2006;58:1185–92.
18. Firsov, AA et al. Testing the mutant selection window hypothesis with *Staphylococcus aureus* exposed to linezolid in an in vitro dynamic model. J. Antimicrob. Chemother. 2017. https://doi.org/10.1093/jac/dkx249.
19. Firsov AA, et al. Enrichment of resistant *Staphylococcus aureus* at ciprofloxacin concentrations simulated within the mutant selection window: bolus versus continuous infusion. Int J Antimicrob Agents. 2008;32:488–93.
20. Firsov AA, Vostrov SN, Lubenko IY, Zinner SH, Portnoy YA. Concentration-dependent changes in the susceptibility and killing of *Staphylococcus aureus* in an in vitro dynamic model that simulates normal and impaired gatifloxacin elimination. Int J Antimicrob Agents. 2004;23:60–66.
21. Cui J, et al. The mutant selection window in rabbits infected with *Staphylococcus aureus*. J Infect Dis. 2006;194:1601–8.
22. Croisier D, et al. *In vivo* pharmacodynamic efficacy of gatifloxacin against *Streptococcus pneumoniae* in an experimental model of pneumonia: impact of the low levels of fluoroquinolone resistance on the enrichment of resistant mutants. J Antimicrob Chemother. 2004;54:640–7.
23. Campion JJ, McNamara PJ, Evans ME. Evolution of ciprofloxacin-resistant *Staphylococcus aureus* in in vitro pharmacokinetic environments. Antimicrob Agents Chemother. 2004;48:4733–44.
24. Olofsson SK, Marcusson LL, Lindgren PK, Hughes D, Cars O. Selection of ciprofloxacin resistance of *Escherichia coli* in an in vitro kinetic model: relation between drug exposure and mutant prevention concentration. J Antimicrob Chemother. 2006;57:1116–21.
25. Gumbo T, et al. Isoniazid bactericidal activity and resistance emergence: integrating pharmacodynamics and pharmacogenomics to predict efficacy in different ethnic populations. Antimicrob Agents Chemother. 2007;51:2329–936.
26. Homma T, Hori T, Sugimori G, Yamano Y. Pharmacodynamic assessment based on mutant prevention concentrations of fluoroquinolones to prevent the emergence of resistant mutants of *Streptococcus pneumoniae*. Antimicrob Agents Chemother. 2007;51:3810–5.
27. Kesteman AS, et al. Influence of inoculum size and marbofloxacin plasma exposure on the amplification of resistant subpopulations of *Klebsiella pneumoniae* in a rat lung infection model. Antimicrob Agents Chemother. 2009;53:4740–8.

28. Li X, et al. Evaluation of meropenem regimens suppressing emergence of resistance in *Acinetobacter baumannii* with human simulated exposure in an *in vitro* intravenous-infusion hollow-fiber infection model. Antimicrob Agents Chemother. 2014;58:6773–81.
29. Zinner SH, Gilbert D, Greer K, Portnoy YA, Firsov AA. Concentration-resistance relationships with *Pseudomonas aeruginosa* exposed to doripenem and ciprofloxacin in an in vitro model. J Antimicrob Chemother. 2013;68:881–7.
30. Kuroda M, et al. Whole genome sequencing of meticillin-resistant *Staphylococcus aureus*. Lancet. 2001;357:1225–40.
31. Stalker DJ, Jungbluth GL. Clinical pharmacokinetics of linezolid, a novel oxazolidinone antibacterial. Clin Pharmacokinet. 2003;42:1129–40.
32. Meaghe AK, Forrest A, Rayner CR, Birmingham MC, Schentag JJ. Population pharmacokinetics of linezolid in patients treated in a compassionate-use program. Antimicrob Agents Chemother. 2003;47:548–53.
33. Firsov AA, et al. In vitro resistance studies with bacteria that exhibit low mutation frequencies: prediction of "antimutant" linezolid concentrations using a mixed inoculum containing both susceptible and resistant *Staphylococcus aureus*. Antimicrob Agents Chemother. 2015;59:1014–9.
34. Smirnova MV, et al. The antistaphylococcal pharmacodynamics of linezolid alone and in combination with doxycycline in an in vitro dynamic model. J Chemother. 2011;23:140–2.
35. Firsov AA, Lubenko IY, Smirnova MV, Strukova EN, Zinner SH. Enrichment of fluoroquinolone-resistant *Staphylococcus aureus*: oscillating ciprofloxacin concentrations simulated at the upper and lower portions of the mutant selection window. Antimicrob Agents Chemother. 2008;52:1924–8.